

Purdue University

Purdue e-Pubs

---

Department of Computer Science Technical  
Reports

Department of Computer Science

---

1999

## 2D-Pattern Matching Image and Video Compression: Theory, Algorithms, and Experiments

Marc Alzina

Wojciech Szpankowski  
*Purdue University, spa@cs.purdue.edu*

Ananth Y. Grama  
*Purdue University, ayg@cs.purdue.edu*

Report Number:

99-010

---

Alzina, Marc; Szpankowski, Wojciech; and Grama, Ananth Y., "2D-Pattern Matching Image and Video Compression: Theory, Algorithms, and Experiments" (1999). *Department of Computer Science Technical Reports*. Paper 1441.

<https://docs.lib.purdue.edu/cstech/1441>

This document has been made available through Purdue e-Pubs, a service of the Purdue University Libraries.  
Please contact [epubs@purdue.edu](mailto:epubs@purdue.edu) for additional information.

**2-D PATTERN MATCHING IMAGE  
AND VIDEO COMPRESSION:  
THEORY, ALGORITHMS AND EXPERIMENTS**

**Marc Alzina  
Wojciech Szpankowski  
Ananth Grama**

**CSD-TR #99-010  
April 1999**

# 2D-Pattern Matching Image and Video Compression: Theory, Algorithms, and Experiments

April 5, 1999

Marc Alzina  
ENST  
46 Rue Barrault  
75013 Paris  
FRANCE  
alzina@email.enst.fr

Wojciech Szpankowski\*  
Dept. of Computer Science  
Purdue University  
W. Lafayette, IN 47907  
U.S.A.  
spa@cs.purdue.edu

Ananth Grama†  
Dept. of Computer Science  
Purdue University  
W. Lafayette, IN 47907  
U.S.A.  
ayg@cs.purdue.edu

## Abstract

In this paper, we propose a lossy data compression framework based on an approximate two dimensional pattern matching (2D-PMC) extension of the Lempel-Ziv lossless scheme. This framework forms the basis upon which higher level schemes relying on differential coding, frequency domain techniques, prediction, and other methods can be built. We apply our pattern matching framework to image and video compression and report on theoretical and experimental results. Theoretically, we show that the *fixed database model* used for video compression leads to suboptimal but computationally efficient performance. The compression ratio of this model is shown to tend to the generalized entropy defined in this paper. For image compression we use a *growing database* model for which we provide an approximate analysis. The implementation of 2D-PMC is a challenging problem from the algorithmic point of view. We use a range of techniques and data structures such as  $k$ -d trees, generalized run length coding, adaptive arithmetic coding, and variable and adaptive maximum distortion level to achieve good compression ratios at high compression speeds. We demonstrate bit rates in the range of 0.25 – 0.5 bpp for high quality images and data rates in the range of 0.15 – 0.5 Mbps for a baseline video compression scheme that does not use any prediction or interpolation. We also show that this asymmetric compression scheme is capable of extremely fast decompression making it particularly suitable for networked multimedia applications.

**Index Terms:** Multimedia compression, approximate pattern matching, Lempel-Ziv schemes, rate distortion, generalized Shannon entropy,  $k$ -d trees, generalized run-length coding, arithmetic coding.

---

\*This work was supported by NSF Grants NCR-9415491 and C-CR-9804760, and Purdue GIFC Grant.

†This work was supported by NSF Grants ACI-9872101 and EIA-9806741.

## 1 Introduction

Lossless data compression based on *exact* pattern matching can be traced back to seminal papers of Lempel and Ziv [22, 23]. More recently, there has been a resurgence of interest in extending these schemes to lossy data compression (cf. [1, 2, 3, 4, 10, 12, 14, 15, 17, 18, 19, 20]). This can be largely attributed to the rapid growth in *digital* representation of multimedia (e.g., text, audio, image, video, etc.) which is particularly amenable to exact and *approximate* pattern matching manipulations.

We believe that the first implementation of lossy image compression based on approximate pattern matching (i.e., a combination of vector quantization and lossy LZ78) was reported by Constantinescu and Storer [3]. Unfortunately, no theoretical justification was provided for this scheme and experimental results were preliminary. The key issue of whether such a scheme is asymptotically optimal (like its lossless Lempel-Ziv counterpart) was first addressed by Steinberg and Gutman [17], and eventually resolved independently by Luczak and Szpankowski [14, 15] and Yang and Kieffer [19]. They proved that a straightforward lossy extension of Lempel-Ziv scheme is not asymptotically optimal. It was demonstrated that the compression bit rate asymptotically achieves the *generalized Shannon entropy*, which is higher than the optimal rate distortion function. More recently, Kontoyiannis [12] proposed a scheme based on approximate pattern matching that is asymptotically optimal for memoryless sources. However, it is not yet clear if this would lead to an implementable solution. Other optimal schemes have been proposed by Zamir and Rose [20] and Zhang and Wei [21].

The central theme of a lossy extension of Lempel-Ziv algorithm is the notion of approximate repetitiveness. If a portion of data recurs in an approximate sense, then subsequent occurrences can be stored as direct or indirect references to the first occurrence. This approximate recurrence of data may not be contiguous. Somewhat surprisingly, this theme of exploiting approximate repetitiveness is uniformly applicable to multimedia data from various sources such as text, images, video, and even audio. However, approximate repetitiveness can be hidden in various forms for different types of media. Therefore, one must consider different distortion measures. This is in contrast with current state-of-the-art, where a different approach is used for compressing each of these types of data.

Using the theoretical underpinning of Luczak and Szpankowski [15], Atallah, Génin and Szpankowski [2] implemented a lossy scheme for image compression. This scheme, called *Pattern Matching Image Compression* (PMIC), was based on *one-dimensional* pattern matching, enhanced with some salient features. It was shown that for high quality

images, the PMIC scheme is competitive with JPEG and wavelet image compression up to 1 bpp. However, the superiority of PMIC at decompression (PMIC does not require any computation since it basically only reads data) may turn out to be a crucial advantage in practice where asymmetric compression/decompression is a desirable feature (e.g., video). *However*, a bit rate of 1 bpp is not that interesting from a practical point of view since most image compression applications require bit rates of 0.5 bpp to 0.25 bpp. In this paper, we describe a new implementation based on two-dimensional approximate pattern matching that achieves compression of up to 0.25 bpp for images while preserving other desirable properties of PMIC. We call this scheme 2D-PMIC for image compression, while for general multimedia compression we coin the term 2D- Pattern Matching Compression (2D-PMC). We also use this idea to develop a new compression scheme for video data that uses the previous frame as the database. Our preliminary experimental results exceed even our expectations: we obtain high quality video with bit rates of 0.15 – 0.5 Mbps (without the first frame). We should underline that this scheme does not use any prediction, interpolation, differential coding, frequency domain transforms, or quantizations. When combined with all these other optimizations, the pattern matching framework is expected to yield even higher compression rates. We report on our theoretical and experimental findings in this paper. The reader is referred to <http://www.cs.purdue.edu/homes/spa/Compression/2D-PMC.html> for image and video compression samples and results.

In this paper, we first discuss the theoretical underpinnings of our scheme and subsequently present algorithmic and experimental results. Our video compression scheme is modeled well by the *fixed database model*. In this model, the first frame serves as a fixed database (reference) for compressing subsequent frames using approximate pattern matching. For this model, we report a theoretical asymptotic bit rate which turns out to be the generalized Shannon entropy. While the generalized Shannon entropy is higher than the optimal rate distortion function, we observe that at least for memoryless sources these two rates do not differ by much (cf. [15]). Our scheme for compressing image data can be modeled using a *growing database* formed by the continually changing reference corresponding to segments of the image that have been compressed. Precise asymptotic analysis of this scheme is beyond the current state-of-the-art. However, we propose an approximate analysis here and expect to derive a more rigorous one in the future.

The implementation of 2D-PMC is a challenging problem from the algorithmic standpoint. Finding an efficient data structure for *approximate* search of multidimensional sets in large databases is an interesting problem in itself. We use a set of modified  $k$ -d trees enhanced by generalized run length coding for approximate search. A key issue for high

quality image and video compression is the design of an adaptive distortion measure that automatically adjusts its maximum distortion to produce perceptually high quality results. We propose a few solutions and examine their performance in this paper.

## 2 Theoretical Underpinnings

Consider a source sequence  $\{X_k\}_{k=1}^{\infty}$  taking values from a finite alphabet  $\mathcal{A}$  (e.g.,  $|\mathcal{A}| = 256$ ). That is,  $X_i : \mathcal{S} \rightarrow \mathcal{A}$  where  $\mathcal{S}$  is a two-dimensional area (e.g., for images  $\mathcal{S}$  is an  $N \times N$  square of pixels). We write  $X_m^n = X_m X_{m+1} \dots X_n$ , and  $P(x_1^n)$  for the probability of  $X_1^n = x_1^n$ . We encode  $X_1^n$  into a compression code  $c_n$ , and the decoder produces an estimate  $\hat{X}_1^n$  of  $X_1^n$ . More precisely, code  $c_n$  is a function  $\phi : \mathcal{A}^n \rightarrow \{0, 1\}^*$ , thus,  $c_n = \phi(x_1^n)$ , where lower-case letters represent realizations of a stochastic process. On the decoding side, the decoder function  $\psi : \{0, 1\}^* \rightarrow \mathcal{A}^n$  is applied to find  $\hat{x}_1^n = \psi(c_n)$ . Let  $\ell(c_n)$  be the length of a code (in bits) representing  $x_1^n$ . Then, the *bit rate* is defined as  $r(x_1^n) = \ell(c_n)/n$ , the *average* bit rate as  $\mathbf{E}[r(X_1^n)] = \mathbf{E}[\ell(C_n)]/n$ , and the *compression ratio*  $CR$  as  $CR = n \log_2 |\mathcal{A}| / \ell(c_n)$ .

We consider *single-letter fidelity* distortion measures  $d : \mathcal{A} \times \hat{\mathcal{A}} \rightarrow \mathbb{R}_+$  such that

$$d(x_1^n, \hat{x}_1^n) = \frac{1}{n} \sum_{i=1}^n d(x_i, \hat{x}_i) ,$$

which is assumed to be subadditive, that is, for any two integers  $n, m$ , and given vectors  $x_1^{n+m}, y_1^{n+m}$

$$d(x_1^{n+m}, y_1^{n+m}) \leq \frac{n}{n+m} d(x_1^n, y_1^n) + \frac{m}{n+m} d(x_{n+1}^{n+m}, y_{n+1}^{n+m}) .$$

Examples of fidelity measures satisfying the above criteria include the *Hamming distance* and the *squared error distortion*. In Hamming distance,  $d(x_i, \hat{x}_i)$  equals zero if  $x_i = \hat{x}_i$  and one otherwise; and in squared error distortion,  $d(x_i, \hat{x}_i) = (x_i - \hat{x}_i)^2$ . Our original PMIC was based on square error distortion, which is natural for image compression. In the current implementation we develop several novel distortion measures that adjust their maximum value to produce the best possible perceptual results.

### 2.1 Fixed Database Model

Our implementation of pattern matching video compression is modeled well by the fixed database scheme. In this scheme, the decoder and the encoder both have access to the common database sequence  $\hat{X}_1^n$  (e.g., the first image in the video stream) generated according to the distribution  $\hat{P}$ . The source sequence  $X_1^M$  (where  $M = N^2$  for  $N \times N$  images)

is partitioned according to  $\Pi_n$  into variable length phrases (e.g., rectangles in 2D-PMC)  $Z^1, Z^2, \dots, Z^{|\Pi_n|}$  of lengths  $L_n^1, \dots, L_n^{|\Pi_n|}$ , respectively. Here, for given fixed distortion bound  $D > 0$

$$\begin{aligned} L_n^1 &= \max\{k : d(\hat{X}_i^{i+k-1}, X_1^k) \leq D, \ 1 \leq i \leq n - k + 1\}, \\ Z^1 &= X_1^{L_n^1}. \end{aligned}$$

This implies that the first partition comprises of the longest prefix of the input  $X_1^M$  that matches a substring in the database  $\hat{X}_1^n$  to the specified tolerance. The string  $\hat{Z}^1$  recovered by the decoder is therefore given by:

$$\hat{Z}^1 = \hat{X}_i^{i+L_n^1-1},$$

Subsequent partitions are computed in a similar manner. That is, if one sets  $K_n(m) = \sum_{i=1}^m L_n^i$ , the  $(m+1)$ -st phrase of partition  $\Pi_n$  is defined as:

$$\begin{aligned} L_n^{m+1} &= \max\{k : d(\hat{X}_i^{i+k-1}, X_{K_n(m)+1}^{K_n(m)+k}) \leq D, \ 1 \leq i \leq n - k + 1\}, \\ Z^{m+1} &= X_{K_n(m)+1}^{K_n(m)+L_n^{m+1}}, \\ \hat{Z}^{m+1} &= \hat{X}_i^{i+L_n^{m+1}-1}. \end{aligned}$$

Thus, the source sequence is partitioned according to  $\Pi_n$  as  $X_1^M = Z^1 Z^2 \dots Z^{|\Pi_n|}$  while the decoder recovers the string  $\hat{Z}^1 \hat{Z}^2 \dots \hat{Z}^{|\Pi_n|}$  which is within distortion  $D$  from  $X_1^M$ . This follows from the subadditive property of the distortion measure. We represent each  $\hat{Z}^i$  by a pointer ptr to the database and its length (recall that  $\hat{Z}^i$  is defined over a two-dimensional domain), hence its description costs  $O(\log n + \log(L_n^i))$  bits. The total compressed code length is

$$\ell_n(X_1^M) = \sum_{i=1}^{|\Pi_n|} \log n + \Theta(\log L_n^i),$$

and the bit rate (in bits per pixel) is given by

$$r_n(X_1^M) = \frac{1}{M} \sum_{i=1}^{|\Pi_n|} \log n + \Theta(\log L_n^i). \quad (1)$$

To formulate our main result, we introduce the generalized Shannon entropy  $\hat{r}_0(D)$  defined as (cf. [15])

$$\hat{r}_0(D) = \lim_{n \rightarrow \infty} \frac{\mathbf{E}_P[-\log \hat{P}(B_D(X_1^n))]}{n}, \quad (2)$$

where  $B_D(\hat{x}_1^n) = \{y_1^n : d(\hat{x}_1^n, y_1^n) \leq D\}$  is the ball of radius  $D$  and center  $\hat{x}_1^n$ , and  $\mathbf{E}_P$  denotes the expectation with respect to  $P$ . We shall prove the following result that provides a theoretical justification for the video scheme considered in this paper.

**Theorem 1** *Let us consider the fixed database model with the database  $\hat{X}_1^n$  generated by a Markovian source  $\hat{P}$  and the source sequence  $X_1^M$  emitted by a Markovian source  $P$ .*

(i) *The length  $L_n^1$  of the first phrase satisfies*

$$\lim_{n \rightarrow \infty} \frac{L_n^1}{\log n} = \frac{1}{\hat{r}_0(D)}, \quad (\text{pr.}). \quad (3)$$

*More precisely, for any  $\varepsilon > 0$*

$$\Pr \left\{ (1 - \varepsilon) \frac{1}{\hat{r}_0(D)} \log n \leq L_n^1 \leq (1 + \varepsilon) \frac{1}{\hat{r}_0(D)} \log n \right\} = 1 - O\left(\frac{\log n}{n^\varepsilon}\right). \quad (4)$$

(ii) *The average bit rate attains asymptotically*

$$\lim_{n \rightarrow \infty} \lim_{M \rightarrow \infty} \mathbf{E}_P[r_n(X_1^M)] = \hat{r}_0(D). \quad (5)$$

**Proof.** We observe that (4) follows directly from [15] for mixing sequences, thus it applies to our situation. We use it in establishing lower and upper bounds. For a lower bound; we define  $\mathcal{H}$  to be a set of those phrases whose length is not bigger than  $(1 + \varepsilon) \frac{1}{\hat{r}_0(D)} \log n$ . Clearly,

$$|\mathcal{H}| \geq \frac{M \hat{r}_0(D)}{(1 + \varepsilon) \log n},$$

which implies

$$r_n(X_1^M) \geq \frac{1}{M} \sum_{\mathcal{H}} \log n \geq (1 - \varepsilon) \hat{r}_0(D).$$

We derive now the matching upper bound. We shall apply the approach suggested in [12, 18]. Let us partition all phrases into “long” phrases and “short” phrases. A phrase  $i$  is long if  $L_n^i \geq (1 - \varepsilon) \log n$  for any  $\varepsilon > 0$ ; otherwise it is a short phrase. Let  $\mathcal{L}_M$  and  $\mathcal{S}_M$  be the sets of long and short phrases, respectively. Observe that

$$N = |\mathcal{L}_M| \leq \frac{M(\hat{r}_0(D))}{(1 - \varepsilon) \log n}. \quad (6)$$

Now we proceed as follows (below  $c$  is a constant that can change from line to line):

$$\begin{aligned} r_n(X_1^N) &\leq \frac{1}{M} \sum_{i \in \mathcal{L}_M} (\log n + c \log L_n^i) + \frac{1}{M} \sum_{i \in \mathcal{S}_M} (\log n + c \log L_n^i) \\ &\stackrel{(6)}{\leq} (1 + \varepsilon) \hat{r}_0(D) + c \frac{N}{M} \sum_{i \in \mathcal{L}_M} \frac{1}{N} \log L_n^i + \frac{1}{M} \sum_{i \in \mathcal{S}_M} (\log n + c \log L_n^i) \\ &\stackrel{\text{Jensen}}{\leq} (1 + \varepsilon) \hat{r}_0(D) + c \frac{N}{M} \log \left( \frac{1}{N} \sum_{i \in \mathcal{L}_M} L_n^i \right) + \frac{1}{M} \sum_{i \in \mathcal{S}_M} (\log n + c \log L_n^i) \\ &\leq (1 + \varepsilon) \hat{r}_0(D) + c \frac{N}{M} \log \left( \frac{M}{N} \right) + \frac{1}{M} \sum_{i \in \mathcal{S}_M} (\log n + c \log L_n^i) \\ &\leq (1 + \varepsilon) \hat{r}_0(D) + \frac{c \log \log n}{\log n} + \frac{1}{M} \sum_{i \in \mathcal{S}_M} (\log n + c \log L_n^i). \end{aligned}$$

We now evaluate the expected value of the third term above (as always, we write  $I(\cdot)$  for the indicator function).

$$\begin{aligned}
\mathbf{E} \left[ \frac{1}{M} \sum_{i \in \mathcal{S}_M} (\log n + c \log L_n^i) \right] &\stackrel{(6)}{\leq} \frac{c}{M} \log n \mathbf{E} \left[ \sum_{i=1}^{|\Pi_n|} I(L_n^i \text{ is short}) \right] \\
&\leq \frac{c}{M} \log n \mathbf{E} \left[ \sum_{i=1}^M I(L_n^1 \text{ is short}) \right] \\
&\leq c \log n \Pr \left\{ L_n^1 \leq (1 - \varepsilon) \frac{1}{\hat{r}_0(D)} \log n \right\} \\
&\stackrel{(4)}{\leq} c \frac{\log^2 n}{n^\varepsilon}
\end{aligned}$$

where the second inequality above follows by considering not just  $i$  but all possible positions on  $X_1^M$  where a short match can occur. Thus

$$\limsup_{n \rightarrow \infty} \limsup_{M \rightarrow \infty} \mathbf{E}[r_n(X_1^M)] \leq \hat{r}_0(D),$$

and this completes the proof. ■

We should point out that  $\hat{r}_0(D) \geq R(D)$  where  $R(D)$  is the optimal rate distortion function. In [15] we observe, at least for memoryless sources, that  $\hat{r}_0(D)$  and  $R(D)$  do not differ by much for moderate values of  $D$ .

## 2.2 Growing Database Model

In contrast to video compression where a reference frame acts as the database, image compression uses the most recent partial compressed image as a (variable) database. This can be modeled by the *growing database model*. Let us assume that the source sequence  $\{X_k\}_{k=1}^\infty$  is generated according to a distribution  $P$ . We set the initial reproduction sequence of length  $m$  to be the same as the first  $m$  symbols of the database, that is,  $X_1^m = \hat{X}_1^m$ . We reveal  $X_1^m$  to the decoder (e.g., in a lossless transmission).

Set  $\hat{X}^0 = X_1^m$  and let  $n_0 = m$ . The algorithm works as follows:

- Find the first match of length  $L_{n_0}^1$  as follows

$$L_{n_0}^1 = \max\{t : d(\hat{X}_i^{i+t-1}, X_{n_0+1}^{n_0+t}) \leq D, \quad 1 \leq i \leq n_0 - t + 1\}.$$

Encode pointer  $\text{ptr}(1) = i$  and the length  $L_{n_0}^1$ . Then we enlarge the database

$$\hat{X}^1 = \hat{X}^0 \star \hat{X}_{\text{ptr}(1)}^{\text{ptr}(1) + L_{n_0}^1 - 1}.$$

where  $\star$  means concatenation. Observe that we do *not* concatenate  $X_{m+1}^{n+L_{n_0}^1}$  but the *distorted* database  $\hat{X}_{\text{ptr}(1)}^{\text{ptr}(1)+L_{n_0}^1-1}$  so that the errors do not propagate. In this case,  $d(X_1^{m+L_{n_0}^1}, \hat{X}_1^{m+L_{n_0}^1}) \leq D$ , as required.

- Provided  $k$ th reproduction sequence  $\hat{X}^k$  of length  $n_k = |\hat{X}^k|$  was constructed, define the  $(k+1)$ -st match length as

$$L_{n_k}^{k+1} = \max\{t : d(\hat{X}_i^{i+t-1}, X_{n_k+1}^{n_k+t}) \leq D, \quad 1 \leq i \leq n_k - t + 1\},$$

and set  $\text{ptr}(k+1) = i$ . The corresponding code is  $(\text{ptr}(k+1), L_{n_k}^{k+1})$ . The enlarged database now becomes

$$\hat{X}^{k+1} = \hat{X}^k \star \hat{X}_{\text{ptr}(k)}^{\text{ptr}(k)+L_{n_k}^{k+1}-1}.$$

As before, by finding the largest match in the *distorted* database, we assure that errors are not propagated, that is,

$$d(X_1^{n_k}, \hat{X}^k) \leq D.$$

for given  $D > 0$ . □

Now, we are in position to define the *operational bit rate* at step  $k$  of the algorithm as

$$r_m(X_m^{n_k}) = \frac{\log n_0 + \log n_1 + \dots + \log n_{k-1} + \Theta(\log L_{n_0}^1) + \dots + \Theta(\log L_{n_{k-1}}^k)}{L_{n_0}^1 + L_{n_1}^2 + \dots + L_{n_{k-1}}^k}. \quad (7)$$

The analysis of  $r_m(X_m^{n_k})$  is currently beyond our reach since the distorted database  $\hat{X}^k$  is non-stationary of unknown distribution. Nevertheless, we propose below a heuristic and approximate analysis of  $r_m(X_m^{n_k})$  for large  $m$  and  $k = o(\log m / \log \log m)$ .

Let us start with an observation that in the growing database model consecutive databases  $\hat{X}^0, \hat{X}^1, \dots, \hat{X}^k$  are nonstationary with, say, probability measures  $\hat{P}^0, \hat{P}^1, \dots, \hat{P}^k$  provided they exist. Due to nonstationarity and continually changing nature of the underlying probability, the analysis of such a model is very intricate. However, based on (3) we shall postulate that the longest approximate match  $L_{n_k}^{k+1}(\hat{P}^k)$  is of order  $\frac{1}{\hat{r}_0^k(D)} \log n_k$  where the coefficient  $\hat{r}_0^k(D)$  depends on the probability measure  $\hat{P}^k$ . We formulate this as a hypothesis that must be verified rigorously if one hopes for a precise analysis of the growing database model.

- [H] At step  $k$  of the algorithm, let the database size be  $n_k$  with underlying probability  $\hat{P}^k$ . There exists a constant  $\hat{r}_0^k(D)$  that depends on  $\hat{P}^k$  such that in probability and on average

$$L_{n_k}^{k+1}(\hat{P}^k) \sim \frac{1}{\hat{r}_0^k(D)} \log n_k \quad (8)$$

for  $n_k \rightarrow \infty$ .

Under hypothesis [H] and assumption  $m \rightarrow \infty$ , we derive an approximate formula for the bit rate  $r_m(X_m^{n_k})$ . Observe that

$$\begin{aligned} n_0 &= m, \\ n_k &= n_{k-1} + L_{n_{k-1}}^k(\hat{P}^{k-1}), \quad k \geq 1. \end{aligned}$$

But under [H], we obtain

$$\begin{aligned} \log n_k &= \log m + O\left(\frac{k \log m}{m}\right), \\ L_{n_k}^{k+1}(\hat{P}^k) &= \frac{1}{\hat{r}_0^k(D)} \log m + O\left(\frac{k \log m}{m}\right) \end{aligned}$$

as long as  $m \rightarrow \infty$ . In view of this and (7), we arrive at

$$r_m(X_m^{n_k}) = \frac{k}{\frac{1}{\hat{r}_0^0(D)} + \frac{1}{\hat{r}_0^1(D)} + \cdots + \frac{1}{\hat{r}_0^{k-1}(D)}} + O\left(\frac{k \log \log m}{\log m}\right).$$

Finally,

$$\mathbf{E}[r_m(X_m^{n_k})] \approx \frac{k}{\frac{1}{\hat{r}_0^0(D)} + \frac{1}{\hat{r}_0^1(D)} + \cdots + \frac{1}{\hat{r}_0^{k-1}(D)}} \quad (9)$$

provided  $k = o(\log m / \log \log m)$  and  $m \rightarrow \infty$ .

The above approximate analysis relies crucially on the hypothesis [H]. Its validity depends on how non-stationary the distorted database is. Our preliminary theoretical investigations indicate that one may construct a non-stationary database such that the asymptotic of (8) does not hold, and one must work with  $\limsup$  and  $\liminf$ . But, even if [H] holds, the compression ratio (9) may still not converge as  $k \rightarrow \infty$ . Figure 1 shows the variation of the bit rate during 2D-PMIC (growing database model). The right-hand side plot in Figure 1 indicates that the average bit rate may not converge to a limit.

### 3 Algorithms, Data Structures and Implementation

In this section, we describe algorithmic and implementation issues related to the compression scheme. The scheme relies on a range of techniques centered around 2-D pattern matching used in conjunction with variable adaptive distortion and run-length encoding. The key computational kernel is a  $k$ -d tree based matching heuristic along with a region growing scheme that identifies maximal matches in an image. The corresponding decompression scheme expands matched patterns and run-length encoded segments. Due to its simplicity,

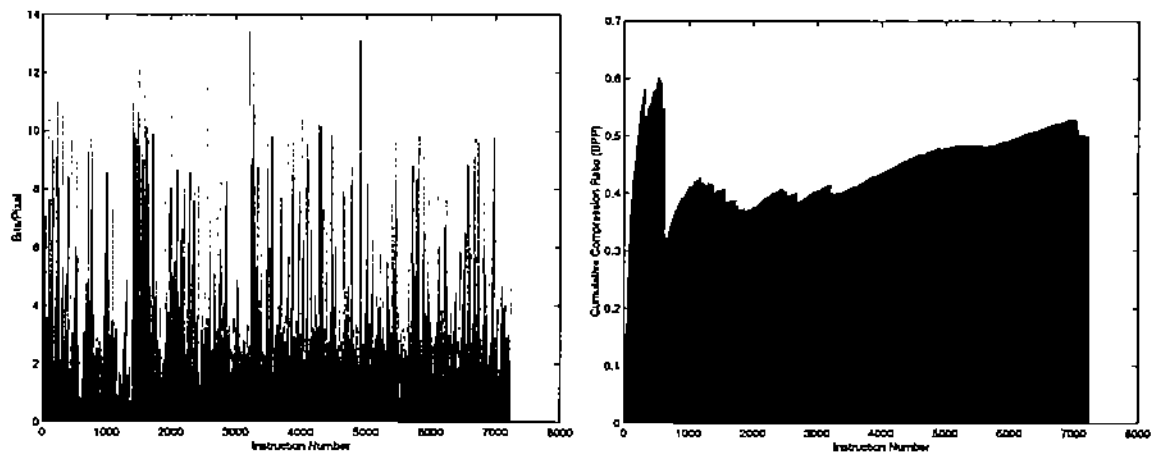


Image Basselope at 0.5 BPP

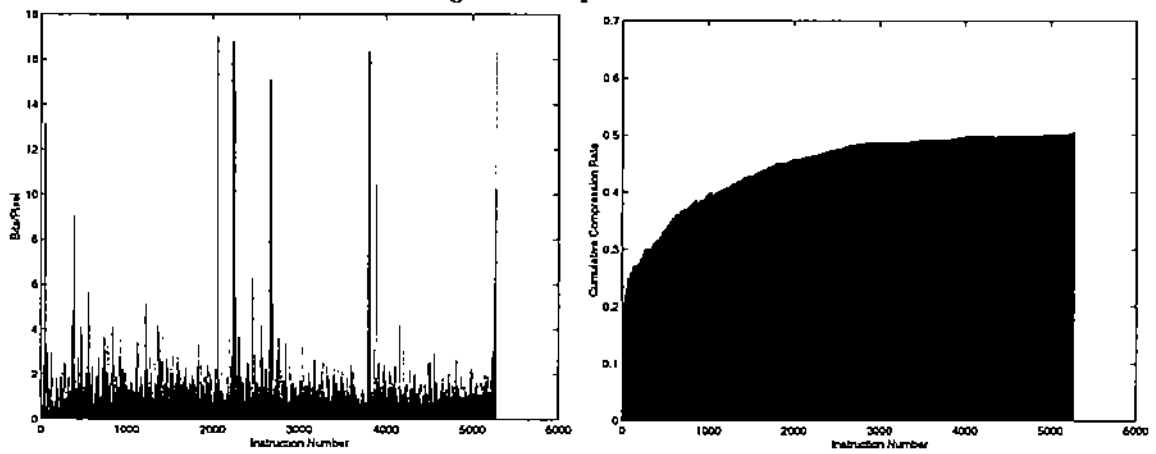


Image Lena at 0.5 BPP

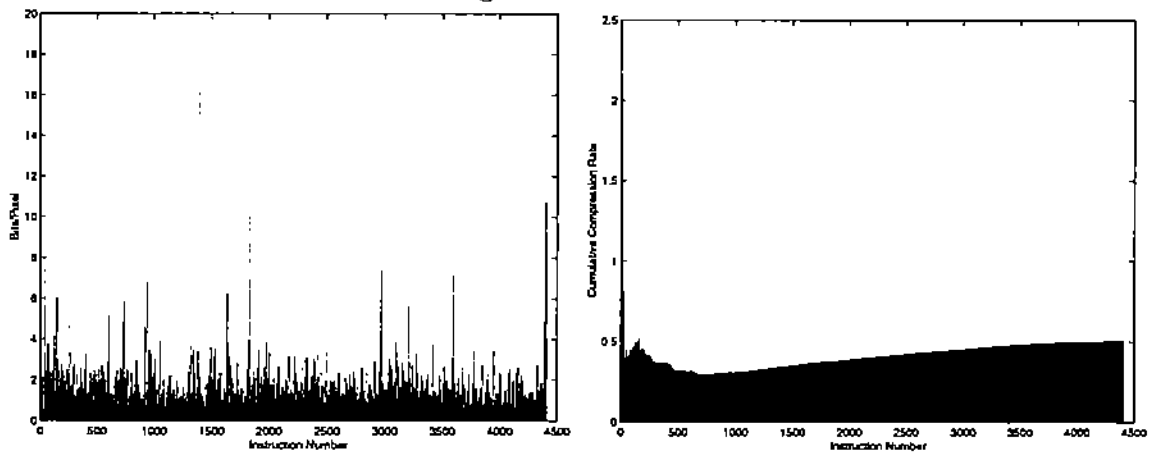


Image San Francisco at 0.5 BPP

Figure 1: Variation of compression rate as the pattern matching process proceeds (Left Column), and Cumulative BPP of the compression process (Right Column).

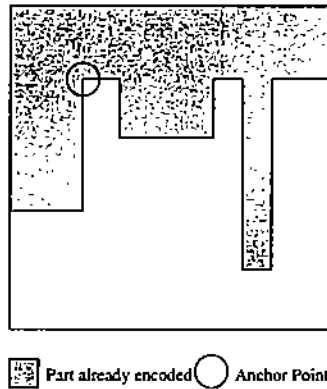


Figure 2: Definition of the Anchor Point

the decompressor runs extremely quickly and requires minimal computation. This is crucial for many applications where one aims to display images and video “on-the-fly” while downloading. This is particularly important for video applications since current schemes (e.g., AVI, QuickTime, MPEG) require significant software support on the decompression side.

The rest of this section addresses the coding techniques based on 2-D matching, run-length encoding, and lossless encoding, distortion metrics, and algorithmic complexities along with implementation details for image and video streams.

### 3.1 Encoding techniques

The compression scheme proposed here uses a combination of three techniques to code data: 2-D pattern matching, enhanced run-length encoding (ERLE), and lossless coding. These techniques are applied to progressively code the image. Assume that a part of an image has been previously encoded. The next step is to encode the pixels located to the right of and below a point we call the *anchor point* (cf. Figure 2). The selection of the next anchor point is based on the *growing heuristic* (cf. [3]). The growing heuristic we adopt is the “wave-front” scheme. This scheme sweeps the image from the top to the bottom of the image. Other heuristics grow regions in a circular manner from a center of the image or expand from the main diagonal. These heuristics have been observed to yield similar results [3]. Once the anchor point has been identified, the partial image is coded using either 2-D pattern matching, ERLE, or lossless coding.

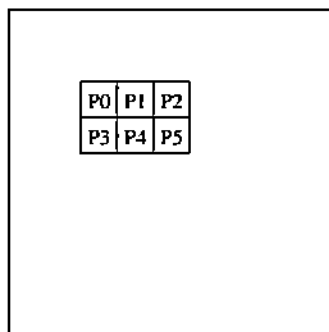


Figure 3: Vector defined by a pixel and a template.

### 3.1.1 Two-Dimensional Pattern Matching

Two dimensional pattern matching is the most efficient way of compressing images among the methods we use in 2D-PMC. The basic idea is to find a two-dimensional region (rectangle) in the uncompressed part of the image that occurs approximately in the compressed part (i.e., database), and to store a pointer to it along with the width and the length of the repeated rectangle. The notion of approximate occurrence is discussed in greater detail in Section 3.2 along with distortion measures. Observe that the objective is to search for the *largest* such area. Consequently, a brute force search algorithm is too time consuming. Indeed, if the database has  $n \times n$  pixels and the as-yet uncompressed region contains  $m \times m$  pixels, then the complexity of the algorithm is  $O(n^2m^2)$ . This is too expensive since we have to apply it approximately  $O(N^2/\log N)$  times on an  $N \times N$  image.

The notion of an approximate occurrence implies that we do not match patterns exactly, rather in an approximate sense. Consequently, we need a *range search* as opposed to an exact search. To accelerate this process, we perform the search in two steps. In the first step, we identify candidate seed points around which a match is possible. In the second step, we grow regions around candidate points and select the largest region matching in the approximate sense.

To identify candidate seed points, we consider a template of  $k$  pixels around the anchor point. Assume that this template is a  $3 \times 2$  region with the anchor point as the top-left pixel in the template. The resulting template corresponds to a 6-dimensional vector (e.g., in Figure 3 the vector associated with  $P_0$  according to the template  $3 \times 2$  of dimension  $k = 6$  is  $(P_0, P_1, P_2, P_3, P_4, P_5)$ ). The problem of finding candidate seed points then becomes one of finding all vectors in a 6-D space that match the vector at the anchor point in an approximate sense.

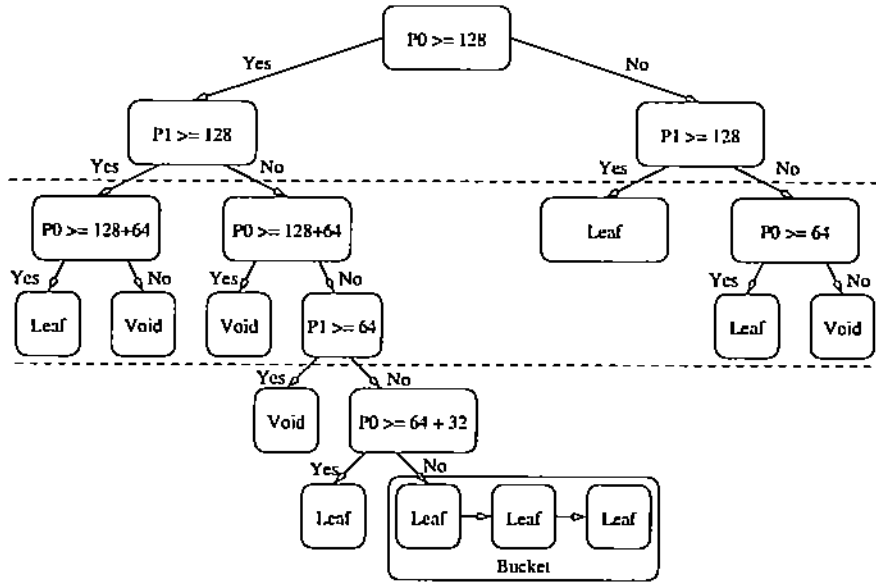


Figure 4: A 2-d-tree (Range 0 – 255)

Search for template matches is performed using  $k$ -d trees (cf. [13, 7]). A 1-D tree is an ordinary binary search tree; a 2-D tree is similar, but the nodes at even levels compare  $x$ -coordinates and the nodes on odd-levels compare  $y$ -coordinates when branching. In general, a  $k$ -d tree has nodes with  $k$  coordinates, and branching at each level is based on only one of the coordinates; for example, we might branch on coordinate number  $(k \bmod l) + 1$  on level  $l$ . Our implementation of  $k$ -d tree search resembles the idea proposed in [3]. To search a  $k$ -dimensional vector using  $k$ -d trees, we trace the tree from the root down to one of the terminal nodes. The decision whether to go left or right at a node is performed on the  $(k \bmod l)$ -th coordinate, where  $l$  is the depth of the node. The terminal nodes are called *buckets* since they contain one or more leaves. Leaf nodes store data corresponding to the vector and coordinates of the associated pixels. An example of a 2-d tree is shown in Figure 4. The height of a tree of  $N$  nodes is bounded to approximately  $\log_2 N$ , and the mean value of the range is used for branching at each node. For example, if the initial range is  $[a, b]$ , the first discriminating value is  $\frac{a+b}{2}$ , the second one (for this coordinate) is  $\frac{a+b}{4}$  (for the left subtree) and  $3\frac{a+b}{4}$  (for the right one), and so on.

To insert a leaf  $L$ , we start from the root and follow the path until we find a bucket  $B$ . There are three possibilities:

- Bucket  $B$  is empty; if so, we insert  $L$  into it.
- The depth of this branch is already equal to the maximum depth  $MaxDepth$ . In this

case, we simply add  $L$  to the bucket which is maintained as a chain of leaves.

- The depth of the node is less than the maximum depth, but the associated bucket  $B$  is full. In this case, we expand the node to its children and select the branching decision as the mean of the node range. All of the leaves in bucket  $B$  are inserted into the buckets at corresponding children and the original leaf  $L$  is re-inserted.

We do a *range search* on a  $k$ -d tree with two arguments: a *minimum* vector  $(m_1, m_2, \dots, m_k)$  and a *maximum* vector  $(M_1, M_2, \dots, M_k)$ . These vectors are determined by the distortion measures discussed in Section 3.2. We search for  $k$ -dimensional vectors  $(v_1, v_2, \dots, v_k)$  such that  $m_1 \leq v_1 \leq M_1, \dots, m_k \leq v_k \leq M_k$ . This is done recursively by keeping every subtree that may contain a solution and discarding the others. For example, if the first discriminating value is 128, then for  $m_1 = 120$  and  $M_1 = 130$  we explore both left and right subtrees of the root, while for  $m = 80$  and  $M = 90$  we just explore the left subtree.

To get an idea about the complexity of this search we first review some known results. Flajolet and Puech [6] presented a very detailed analysis of random  $k$ -d trees. Among other things, they proved that the average search time for a key in a  $k$ -d tree built from  $N$  randomly inserted nodes is

$$\frac{2}{k} \ln N + O(1).$$

However, the situation is more intricate when some (say  $t$ ) coordinates are not specified. Then the search time increases to  $\Theta(N^{1-t/(k+\theta)})$  where  $\theta < 0.06$ . If the  $k$ -d tree is balanced with height  $\approx \log_2 N$ , then Lee and Wong [13] proved that a range search of rectangle areas is bounded by  $O(tN^{1-1/k} + q)$ , where  $t$  of the coordinates are restricted to subranges and there are  $q$  such records. Finally, Friedman et al. [7] showed that if the search area is small and near cubical, then the search time is  $O(\log N + q)$ .

The  $k$ -d tree search used here falls under the model of Friedman et al. [7]. To obtain a more precise estimate of the search time, let us bound the number of paths explored per coordinate assuming the maximum depth is  $d \approx \log_2 N$ , and the search range is  $[\alpha, \beta]$  for every coordinate. The maximum number of subranges that overlap with the search range is  $s = \lceil \frac{(\beta-\alpha)2^d}{b-a} \rceil + 1$ . Thus, for a problem of dimension  $k$ , we must search at most  $s^k$  buckets. A bound for the maximum number of comparisons is  $q = O(ks^k d)$ . For example, for  $b - a = 255$ ,  $\beta - \alpha = 8$ ,  $d = 5$ , and  $k = 6$  we have  $s = 2$  and  $q = 1953$ . In view of this, the total search time is  $O(ks^k \log N)$ . Actual search performance of a  $k$ -d tree is illustrated on the below example:

- dimension:  $k = 6$

- database size:  $262144 = 512 \times 512$  random vectors (8 bits per coordinate)
- maximum tree depth: 30 (5 levels per coordinate)
- solutions found: 72
- search time: 2.7ms (8.11s for 3000 searches) on a PII 300MHz.

However, in order to find all interesting solutions, we actually use several  $k$ -d trees, each one associated with a different template. Furthermore, to decrease the number of potentially non-interesting solutions, pixels and their associated vectors are grouped by locations (by rectangles whose typical size is  $30 \times 30$ ) and one  $k$ -d tree is used per location, so that we can perform a local search.

Our implementation of the  $k$ -d tree follows the idea of [3]. The data structure used to represent a  $k$ -d tree is a set of two arrays:  $A_n$  the array of nodes, and  $A_l$  the array of leaves. A cell,  $A_n$ , is composed of two pointers  $P_l$  and  $P_r$  that can be used differently:

- If  $P_l$  is equal to a special value *IsLeaf*, then the node is actually a leaf, and the contents of the leaf can be found in the cell pointed to by  $P_r$  in  $A_l$ ;
- Else  $P_l$  and  $P_r$  are pointers to the left and right children. A NULL pointer represents an empty bucket.

The structure of a cell of  $A_n$  is as follows:

- The vector used to index the leaf;
- A reference (i.e., the coordinates of the point associated with the color vector);
- A pointer to the next leaf. This is used to chain leaves if the bucket contains more than one leaf.

Finally, the procedure to determine the largest two-dimensional match works as follows: for each template, extract the pixel vector associated to the anchor point and search for similar ones in the  $k$ -d trees containing the pixel vectors of the neighboring locations. For each solution, check if it has already been found by searching with another template. If not, apply the same algorithm as for enhanced run-length encoding (discussed in Section 3.1.2) to find the best match shape. If the number of solutions exceeds a preset limit, we abort the search.

### 3.1.2 Enhanced Run-Length Encoding

Run-length encoding of images identifies regions of the image with constant pixel values. We extend this using a simple variant called enhanced run-length encoding (ERLE). ERLE fits a planar surface on to the given  $m \times n$  grid of pixel values. The coefficients of the planar surface can be determined simply by solving a system of normal equations to minimize least-squared error. Once the planar surface has been determined, the sub-segment of the  $m \times n$  grid that is within the distortion envelope can be identified and coded using ERLE. We have observed that this is particularly useful for synthetic images typically found on web sources.

To identify the largest sub-segment of a given  $m \times n$  grid that can be coded using ERLE, we use the following procedure:

1. Initialize  $x$  to an arbitrary constant, say  $x = 2$ .
2. Test if the rectangle anchored at the *anchor point* of size  $x \times 1$  can be encoded using ERLE with an acceptable quality loss.
3. While step 2 gives a positive answer, double  $x$ .
4. Let  $X$  be the largest  $x$  found through dichotomy for which we can encode the rectangle  $x \times 1$ .
5. Apply the same strategy to find the largest  $Y$ .
6. If  $X \geq Y$ , then for  $y = 2$  to  $Y - 1$  find by dichotomy the greatest  $x$  so that the rectangle  $x \times y$  can be ERL encoded.
7. If  $X < Y$ , swap the role of the  $x$ -coordinate and the  $y$ -coordinate in step 6 above.

When running this algorithm, we compare the cost in terms of the number of bits used to store the ERLE parameters per pixel encoded, of the current and previous solution, and select the better one. Note that the number of bits used is calculated according to the distribution model used by the lossless compressor discussed below. This important fact allows us to save some more memory during the lossless encoding phase.

### 3.1.3 Lossless Encoding

Once the lossy image compression is completed, the image description is a script in the following form: `instruction1, parameters1, instruction2, parameters2, and so on`

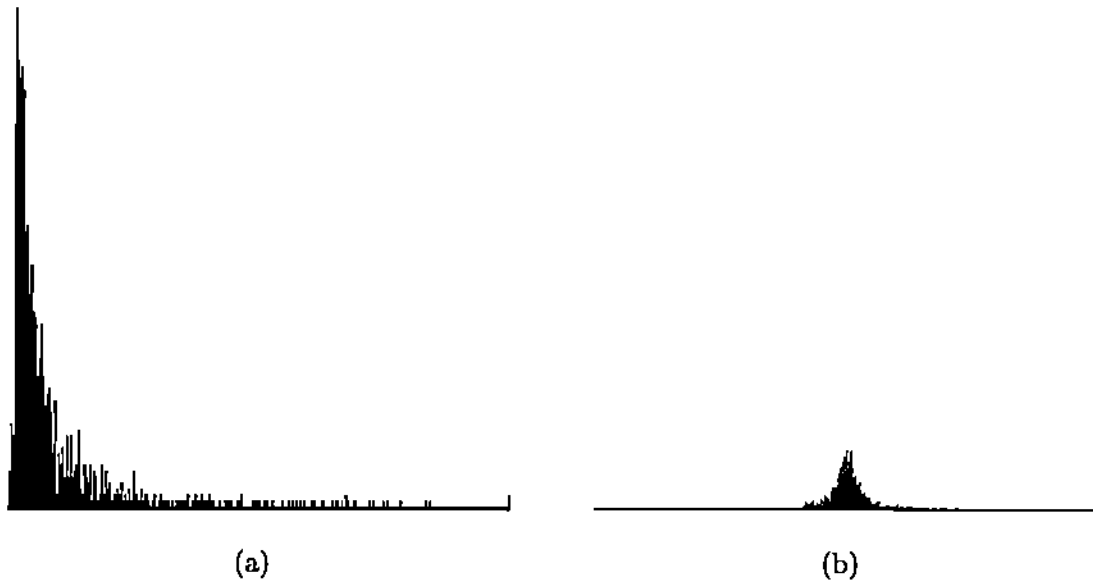


Figure 5: Typical histograms of: (a) the height of matching areas; (b) of the coefficient  $c_0$  in the ERLE coding.

where  $\text{instruction}_N \in \{\text{Pixel\_Color}, \text{Enhanced\_RLE}, \text{Match\_Pointer}\}$  and where the parameter set is different for each instruction. The stream sent to the arithmetic encoder appears as follows:

$$\begin{array}{ccccccc}
 \underbrace{10} & \underbrace{10101001} & \underbrace{00110100100} & \dots & & & \\
 \text{instruction} & \text{parameter}_{10\ 1} & \text{parameter}_{10\ 2} & & & & \\
 \underbrace{01} & \underbrace{0100} & \underbrace{001001} & \dots & & & \\
 \text{instruction} & \text{parameter}_{01\ 1} & \text{parameter}_{01\ 2} & & & & 
 \end{array}$$

with different ranges and distributions for each instruction/parameter.

Since the distribution of the parameter values is not uniform (cf. Figure 5), we can save memory using lossless compression. To make this compression efficient, a distribution model is built for each parameter according to the values it has previously observed, and the stream is encoded using arithmetic coding. Since we want this compression method to be suitable for WWW-based applications, the instruction/parameters are multiplexed in the same arithmetic coding stream, so that the image/video can be displayed on-the-fly while downloading. In fact, we implemented our own arithmetic encoder based on the ideas discussed in [11], hence we refrain from describing it in detail.

## 3.2 Distortion Measures

The process of lossy compression can be viewed as adding “noise” to the image. For this reason, we refer to distortion  $D$  as *RandomNoise*. The original pattern matching scheme PMC [2] computed the distortion-per-symbol for a block of data (averaged over the block). This distortion measure was referred to as *uniform distortion*. We observe experimentally, however, that uniform distortion leads to significant perceptual errors. To avoid this, in 2D-PMC we adopt an alternate approach in which we assign to each *individual* pixel a *range* (i.e., lower and upper bounds on the allowable distortion value per pixel) that depends on the values of surrounding pixels. The basic idea is to be less tolerant (i.e., have a small range) in slowly varying regions and more tolerant in quickly varying regions. We have experimentally evaluated several approaches and describe some of these.

### 3.2.1 Local Distortion Range

In order to reproduce more accurately slowly varying regions, we introduce differences between an individual pixel value and its surrounding neighbors. The range assigned to the pixel located at  $(x, y)$  is given by:

$$\text{Range} = \text{RandomNoise} + \text{LocalNoise} \times \text{LocalVariation}$$

where  $D = \text{RandomNoise}$  is the maximum distortion assigned in the uniform distortion method, *LocalNoise* is additional distortion, and *LocalVariation* is the maximum of the absolute value of the differences between the pixel values at  $(x, y)$  and its 8 neighbors. The drawback of this method is that it deals only with the 8 closest pixels and consequently it is very sensitive to noise.

### 3.2.2 Global Distortion Range

To counter ill effects of the locality of the previous method, we introduce a function that assigns a large range only when there are few pixels of similar value around it. This is computed for pixel  $P_0$  located at  $(x, y)$  as follows (cf. Figure 6):

Define the weight  $W_{ij}$  as

$$W_{ij} = \max\left(0, 1 - \frac{\sqrt{i^2 + j^2}}{r}\right).$$

where  $r = pr\_stretch$  (cf. Figure 6) is the radius of a circle surrounding pixel  $P_0$ . Observe that  $0 \leq W_{ij} \leq 1$ , and its value decreases with the distance from  $P_0$ . Denoting the pixel

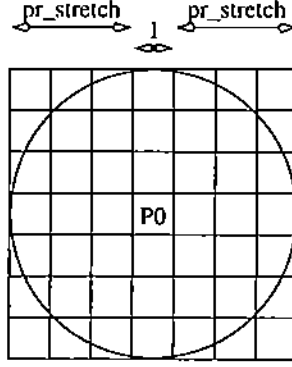


Figure 6: Illustration of the Global Distortion Range ( $pr\_stretch = r$ )

value at location  $(i, j)$  by  $V_{ij}$ , we define  $\delta_{ij}$  as follows:

$$\delta_{ij} = |V_{i+x, j+y} - V_{x,y}|,$$

and the total weight  $W$  as

$$W = \sum_{\substack{0 < |i| \leq r \\ 0 < |j| \leq r}} W_{ij}.$$

We compute the sum  $S$  as

$$S = \frac{pr\_min}{W} \sum_{\substack{0 < |i| \leq r \\ 0 < |j| \leq r}} \frac{W_{ij}}{\min(pr\_max, \max(pr\_min, \delta_{i,j}))}$$

where  $pr\_min$  and  $pr\_max$  are constants. The selection of  $pr\_min$  and  $pr\_max$  is such that we try to assure  $\delta_{ij} \in [pr\_min, pr\_max]$ . The parameter  $S$  should be close to 1 for slowly varying area (c.g., if  $\delta_{ij} = 0$  for all  $i, j$ , then  $S = 1$ ), and  $S$  should be smaller than 1 for quickly changing area. Finally, the range  $R$  for pixel  $P_0 = (x, y)$  is computed as

$$R = RandomNoise + Amplitude \times \left( \frac{1}{S} - pr\_flat \right)$$

where  $pr\_flat$  is chosen close to 1, and  $Amplitude$  is a constant. Thus, the pixel value  $V_{x,y}$  of  $P_0$  can take values in the interval  $[-R + V_{x,y}, R + V_{x,y}]$ .

We observe that the variation in  $R$ , and hence the distribution of errors in this method is less specky than the one computed with the local distortion. This method gives better visual results than the previous one, because it hides the compression noise more efficiently. The difficulty in applying this method lies in tuning the parameters  $pr\_min$ ,  $pr\_max$  and  $Amplitude$  in order to obtain the best visual quality of an image.

Image	BPP	Compr. Time	Decompr. Time
Lena	0.25	108	0.075
	0.5	129	0.153
Basselope	0.27	122	0.106
	0.5	120	0.198
San Francisco	0.25	99	0.061
	0.5	115	0.125
Banner	0.25	8	0.007
	0.5	7	0.010

Table 1: Compression and decompression times (in seconds) for four images on a 400 MHz Pentium II.

### 3.3 Overall Space and Time Complexity

We argue that the overall time complexity of the compression algorithm is optimal and equal to  $O(N^2)$ ; the corresponding decompression time is  $O(N^2/\log N)$ , and the space complexity is  $O(N^2)$ .

Let us first consider the compression algorithm. The most time consuming step is the two-dimensional pattern matching that is approximately applied  $O(N^2/\log N)$  times since we proved that a typical repeated rectangle has  $O(\log N)$  pixels with high probability (and also in the worst case if we restrict the searched area). But, search time in a  $k$ -d tree is also  $O(\log N)$ , hence the total time complexity is  $O(N^2)$ . While this is optimal, the constant in front of  $N^2$  is large due to the many potential searches allowed in the  $k$ -d tree (cf. Section 3.1.1). This constant can be reduced by limiting the search window for potential seed points for pattern matching. Typical compression times for four images are shown in Table 1.

As mentioned before, the decompression is extremely simple and very fast. It requires only  $O(N^2/\log N)$  read operations, and it does not require any additional computation, if the arithmetic coding is not used. This is clearly evidenced by the decompression times in Table 1. The simple and inexpensive decompression scheme allows one to send the decompression program along with the data when downloading images from the web, obviating the need for decoding software on the decompression side.

The space complexity of the technique is  $O(N^2)$ . To get an idea of actual memory requirements,  $k$ -d trees for “Lena”, “Basselope”, and “Banner” require 31.6 MB, 21MB, and 2MB respectively. While most current PCs easily support such memory requirements,

Image #	BPP	CR	RMSE	PSNR
2	0.09	84.9	20.6	21.86
3	0.11	73.9	23.6	20.68
2	0.57	14.0	16.8	23.64
3	0.36	22.3	19.3	22.43

Table 2: Video “Train” with and without model pre-filtering.

these can be further improved. Our implementation maintains  $k$ -d trees corresponding to entire images. However, using the assumption that likely matches are found in the vicinity of the anchor point, we can reduce the space requirement considerably.

### 3.4 Video Implementation

Pattern matching video compression uses the previous compressed frame in its uncompressed form as the database to compress current frame. The reason for this is that we want the uncompressed image at the client side to be within a distortion bound from the original image. Since the decompressor only knows the compressed frame (in its compressed and uncompressed form), this must be used as the database for pattern matching compression. In contrast, if the original previous frame was used as the database, this database is not available at the decompressor. Consequently, errors propagate quickly through subsequent frames during decompression. Since the previous compressed frame (in its uncompressed form) forms a static database, the compression process is modeled well by our analytical framework of Section 2.1.

Applying this framework directly to video compression, it was noticed that the matched patterns were often quite small leading to low compression ratios. This is a consequence of applying distortion (i.e., approximate pattern matching) to *each* individual pixel instead of averaging over the matched area. To circumvent this problem, we apply pattern matching to a low-pass filtered version of the image. In principle, to decide whether or not two areas are alike, we compare their filtered versions. If we find a good match in the filtered image, we apply it to the non-filtered image. Experimental results indicate that for some samples of video for which the compression did not work well (e.g., compression ratio  $\simeq 4$ ) this method could improve the performance enormously (e.g.,  $CR \simeq 50$  video) without noticeable loss in quality. Table 2 compares the compression with and without the low-pass filter.

To implement this idea, we keep two copies of the previous frame. One as it has been encoded, and another that is a filtered version. We also keep at hand a plain and a filtered

version of the image being encoded. We populate the  $k$ -d trees with templates from the filtered version of the previous image. When trying to find a match, we search  $k$ -d trees for a template that is at the location pointed by the anchor point in the filtered image. On finding a match, we store a pointer to it. Notice, however, that during the decoding phase, since the decoder knows nothing about the filtering, it will make a copy of the non filtered pixels. Thus, the image reproduced is still sharp, even if we use a smoothed version to determine “motion vectors”.

The low-pass filtered image is computed using a convolution matrix defined as follows:

$$C = \begin{pmatrix} c_{-1,-1} & c_{-1,0} & c_{-1,+1} \\ c_{0,-1} & c_{0,0} & c_{0,+1} \\ c_{+1,-1} & c_{+1,0} & c_{+1,+1} \end{pmatrix}.$$

That is, the new pixel values  $\tilde{V}_{ij}$  of the smoothed image become

$$\tilde{V}_{i,j} \leftarrow \sum_{-1 \leq k,l \leq 1} V_{i+k,j+l} c_{k,l}$$

where  $V_{ij}$  are pixel values of the original image.

The filters we have tried are:

- A low-pass filter with the frequency response  $h(f_x, f_y) = \left| \frac{(1 + \cos(2\pi f_x))(1 + \cos(2\pi f_y))}{4} \right|$ ,  $0 \leq f_x \leq \frac{1}{2}, 0 \leq f_y \leq \frac{1}{2}$ . The convolution matrix for this filter is:

$$C = \frac{1}{4} \begin{pmatrix} \frac{1}{4} & \frac{1}{2} & \frac{1}{4} \\ \frac{1}{2} & 1 & \frac{1}{2} \\ \frac{1}{4} & \frac{1}{2} & \frac{1}{4} \end{pmatrix}.$$

- A low-pass filter with the frequency response  $h(f_x, f_y) = \left| \frac{(1 + 2 \cos(2\pi f_x))(1 + 2 \cos(2\pi f_y))}{9} \right|$ ,  $0 \leq f_x \leq \frac{1}{2}, 0 \leq f_y \leq \frac{1}{2}$ . The convolution matrix in this case is:

$$C = \frac{1}{9} \begin{pmatrix} 1 & 1 & 1 \\ 1 & 1 & 1 \\ 1 & 1 & 1 \end{pmatrix}.$$

- The same as above, but with matrix  $C$  of dimension 5.

We observed that the second filter yields the best performance.

2D-PMIC				JPEG			
BPP	CR	RMSE	PSNR	BPP	CR	RMSE	PSNR
Image: Banner							
0.29	27.98	9.5	28.6	0.29	27.80	27.4	19.4
0.50	15.99	1.3	45.8	0.50	15.87	15.3	24.5
0.54	14.89	0.0	Inf	1.01	7.94	15.1	24.6
				2.00	4.00	15.1	24.6
Image: Basselope							
0.27	29.56	21.0	21.7	0.25	32.31	19.3	22.4
0.51	15.58	12.6	26.2	0.50	16.17	12.5	26.2
0.96	8.33	0.0	Inf	1.00	7.95	6.9	31.4
				2.01	4.08	2.6	39.7
Image: Lena							
0.25	32.01	10.8	27.5	0.25	32.30	8.9	29.1
0.49	29.30	8.7	29.3	0.50	16.03	5.8	32.9
1.05	7.61	5.6	33.1	1.00	8.04	4.2	35.7
1.94	4.13	3.6	37.1	2.01	3.81	2.7	39.4
Image: San Francisco							
0.25	32.58	17.0	23.5	0.25	31.90	15.5	24.3
0.50	16.09	13.1	25.8	0.50	15.91	10.6	27.6
1.05	7.59	6.7	31.6	1.00	8.02	6.8	31.5
2.03	3.95	2.9	38.8	2.01	3.98	3.5	37.2

Table 3: Comparison of compression results from 2D-PMIC and JPEG for different images.

## 4 Experimental Results

In this section, we present some experimental results for image and video compression. Pattern matching image compression is compared to JPEG compression in Table 3. Several observations can be made from this table:

- For synthetic images (Banner and Basselope), 2D-PMIC outperforms JPEG both in terms of compression ratios as well as quality. This is also evident from Figure 7. A comparison between 2D-PMIC and wavelets shows similarly the superiority of 2D-PMIC [2].
- For compression of general images, 2D-PMIC is competitive with JPEG and wavelet

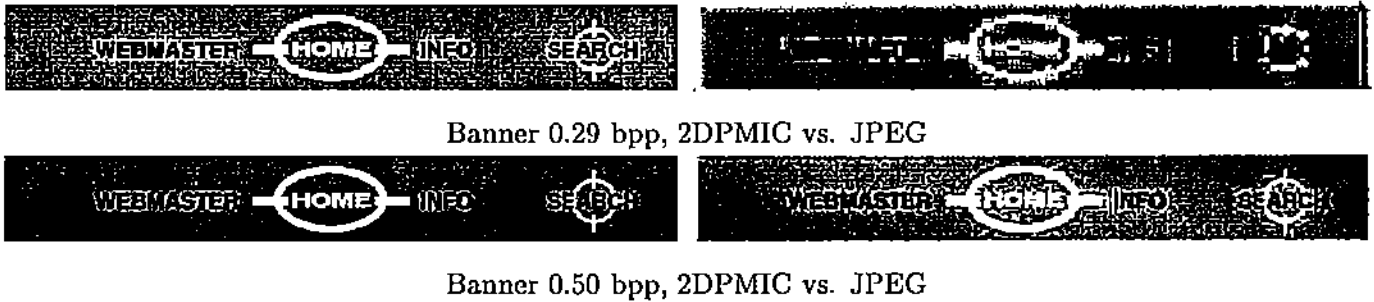


Figure 7: Comparison of image quality using 2D-PMIC and JPEG compression.

compression up to 0.25 bpp.

- At very low bit rates, frequency domain methods are still better than 2D-PMC for natural images.

These results indicate that for synthetic images and higher bit rates, 2D-PMC is the method of choice, particularly because of the simplicity of the decompression procedure.

In Table 4 we show some results of video compression for two video clips, namely “Claire” and “Ping.Pong”. We compress them using 2-D PMC with the previous uncompressed frame as the database. The results presented do not include the first frame and do not make use of any predication (so we really cannot yet talk about a video stream). A demo is set up at <http://www.cs.purdue.edu/homes/spa/Compression/2D-PMC.html> for the reader’s evaluation. Table 4 presents results for “low-quality” (lq) and “high-quality” (hq) compression. It is clear from the table that 2D-PMC yields excellent compression ratios and quality while supporting very high decompression rates. Indeed, by augmenting this technique with inter-frame prediction (in a manner similar to MPEG), the performance can be further enhanced. The objective here however is to demonstrate the power of the pattern matching framework upon which the rest of the conventional compression machinery can build. We are currently working on a Java decompressor that can be transmitted with the compressed video obviating the need for installation of decompression clients.

## 5 Concluding Remarks

In this paper, we have presented a 2D pattern matching framework for compression of image and video data. The following conclusions can be made:

- 2D-PMIC yields excellent compression ratios and is competitive with JPEG and wavelet based compression up to 0.25 bpp. 2D-PMIC works better on synthetic

Video	Mbps	CR	PSNR
Claire_hq	0.14	169	33.7
Claire_lq	0.07	347	31.0
Ping-Pong_hq	0.40	58	24.0
Ping-Pong_lq	0.26	89	22.6

Table 4: Video compression results: low quality (lq) and high quality (hq).

images while transform-based methods work better on natural images. In general, 2D-PMIC works better when high frequency components dominate the image;

- 2D-PMC is slower in terms of compression time but extremely fast and simple in terms of decompression. Decompression can be done on-fly with minimal software support at the client.
- 2D-PMC naturally adapts to variable resource availability by changing the distortion bound. This results in higher compression rates as well as faster compression times.
- The pattern matching framework of 2D-PMC can be used in conjunction with many of the current techniques to leverage the benefits these schemes.

We are currently working on improving the pattern matching framework and combining it with other conventional techniques based on frequency domain techniques. More work is needed on automatic selection of parameters for the pattern matching scheme. 2D-PMC for video is particularly promising, and we are exploring it actively as a part of our ongoing research. When applied in conjunction with prediction and frequency transforms, our framework has the potential to yield significantly improved performance. Alternately, the pattern matching framework can itself be used as a homogeneous compression technique for textual, audio, image, and video data leading to a uniform multimedia compression standard.

## ACKNOWLEDGEMENT

It is our privilege to acknowledge valuable discussions with Y. Reznik (RealNetwork Inc.) and I. Kontoyiannis (Purdue University).

## References

- [1] D. Arnaud and W. Szpankowski, Pattern Matching Image Compression with Prediction Loop: Preliminary Experimental Results, *Proc. Data Compression Conference*, Snowbird 1997; also Purdue University, CSD-TR-96-069, 1996.
- [2] M. Atallah, Y. Génin, and W. Szpankowski, A Pattern Matching Image Compression: Algorithmic and Empirical Results, *IEEE Trans. Pattern Analysis and Machine Intelligence*, to appear; also *Proc. International Conference on Image Processing*, vol. II. 349–352, Laussane 1996.
- [3] C. Constantinescu and J. A. Storer, Improved Techniques for Single-Pass Adaptive Vector Quantization, *Proc. IEEE*, 82, 933–939, 1994.
- [4] A. Dembo and I. Kontoyiannis, The Asymptotics of Waiting Times Between Stationary Processes, Allowing Distortion, *Annals of Applied Probability*, to appear.
- [5] W. Finamore, M. Carvalho, and J. Kieffer, Lossy Compression with the Lempel-Ziv Algorithm, *11th Brazilian Telecommunication Conference*, 141–146, 1993.
- [6] P. Flajolet and P. Puech, Partial Match Retrieval of Multidimensional Data, *J. of the ACM*, 33, 371–407, 1986.
- [7] J. H. Friedman, J. Bentley and R. Finkel, An Algorithm for Finding Best Matches in Logarithmic Expected Time, *ACM Trans. Mathematical Software*, 3, 209–226, 1977.
- [8] A. Gersho and R. Gray, *Vector Quantization and Signal Compression*, Kluwer, 1992.
- [9] J. Gibson, T. Berger, T. Lookabaugh, R. Baker *Multimedia Compression: Applications & Standards*, Morgan Kaufmann Publishers 1998.
- [10] P. G. Howard, Lossless and Lossy Compression of Text Images by Soft Pattern Matching, *Proc. Data Compression Conference*, 210–219, Snowbird 1996.
- [11] P. Howard and J. Vitter, Analysis of Arithmetic Coding for Data Compression, Brown University, Department of Computer Science, *Proc. Data Compression Conference*, 3–12, Snowbird 1991.
- [12] I. Kontoyiannis, An Implementable Lossy Version of the Lempel-Ziv Algorithm— Part I: Optimality for Memoryless Sources, preprint 1998.
- [13] D.T. Lee and C.K. Wong, Worst-Case Analysis for Region and Partial Region Searches in Multidimensional Binary Search Trees and Balanced Quad Trees, *Acta Informatica*, 9, 23–29, 1977.
- [14] T. Luczak and W. Szpankowski, A Lossy Data Compression Based on String Matching: Preliminary Analysis and Suboptimal Algorithms, *Proc. Combinatorial Pattern Matching*, 102–112, Asilomar 1994.
- [15] T. Luczak and W. Szpankowski, A Suboptimal Lossy Data Compression Based in Approximate Pattern Matching, *IEEE Trans. Information Theory*, 43, 1439–1451, 1997.

- [16] M. Rabbani and P. Jones, *Digital Image Compression Techniques*, SPIE Optical Engineering Press, Bellingham 1991.
- [17] Y. Steinberg and M. Gutman, An Algorithm for Source Coding Subject to a Fidelity Criterion, Based on String Matching, *IEEE Trans. Information Theory*, 39, 877-886, 1993.
- [18] A. Wyner and J. Ziv, The Sliding Window Lempel-Ziv algorithm Is Asymptotically Optimal, *Proc. IEEE*, 82, 872-877, 1994.
- [19] E.H. Yang, and J. Kieffer, On the Performance of Data Compression Algorithms Based upon String Matching, *IEEE Trans. Information Theory*, 44, 47-65, 1998.
- [20] R. Zamir and K. Rose, Natural Type Selection in Approximate String Matching, preprint 1999.
- [21] Z. Zhang and V. Wei, An On-Line Universal Lossy Data Compression Algorithm via Continuous Codebook Refinement – Part I: Basic Results, *IEEE Trans. Information Theory*, 42, 803-821, 1996.
- [22] J. Ziv and A. Lempel, A Universal Algorithm for Sequential Data Compression, *IEEE Trans. Information Theory*, 23, 3, 337-343, 1977.
- [23] J. Ziv and A. Lempel, Compression of Individual Sequences via Variable-Rate Coding, *IEEE Trans. Information Theory*, 24, 530-536, 1978.